Function of Partially Duplicated Human α7 Nicotinic Receptor Subunit *CHRFAM7A* Gene.

*POTENTIAL IMPLICATIONS FOR THE CHOLINERGIC ANTI-INFLAMMATORY RESPONSE**

Ana M. de Lucas-Cerrillo[1], M. Constanza Maldifassi[1], Francisco Arnalich[2], Jaime Renart[3], Gema Atienza[1], Rocío Serantes[1,2], Jesús Cruces[3,4], Aurora Sánchez-Pacheco[3,4], Eva Andrés-Mateos[5] and Carmen Montiel[1#]

From [1]Departamentos de Farmacología y Terapéutica, [2]Medicina Interna y [4]Bioquímica. Universidad Autónoma de Madrid. Facultad de Medicina/Hospital La Paz. IdiPAZ. Arzobispo Morcillo 4, 28029 Madrid, Spain. [3]Instituto de Investigaciones Biomédicas "Alberto Sols", CSIC, Arturo Duperier 4, 28029 Madrid, Spain. [5]McKusick-Nathans Institute of Genetic Medicine, Johns Hopkins University School of Medicine, 733 North Broadway Street, Suite 540, Baltimore, MD 21205, USA.

Running Title: Dominant negative effect of dupα7 on α7 receptor activity

[#]Address correspondence to: Carmen Montiel, Departamento de Farmacología y Terapéutica, Facultad de Medicina, Universidad Autónoma de Madrid. Arzobispo Morcillo 4. 28029 Madrid, Spain. Phone: (34) 91-4975390; Fax: (34) 91-4975353. E-mail: carmen.montiel@uam.es

The neuronal α7 nicotinic receptor subunit *gene (CHRNA7)* is partially duplicated in human genome forming a hybrid gene (*CHRFAM7A*) with the novel *FAM7A* gene. The hybrid gene transcript, dupα7, has been identified in brain, immune cells and the HL-60 cell line, although its translation and function are still unknown. In this paper dupα7 cDNA has been cloned and expressed in GH4C1 cells and *Xenopus* oocytes to study the pattern and functional role of the expressed protein. Our results reveal that dupα7 transcript was natively translated in HL-60 cells and heterologously expressed in GH4C1 cells and oocytes. Injection of dupα7 mRNA into oocytes failed to generate functional receptors, but, when co-injected with α7 mRNA, at α7/dupα7 ratios of 5:1, 2:1, 1:1, 1:5 and 1:10, it reduced the nicotine-elicited α7 current generated in control oocytes (α7 alone) by 26%, 53%, 75%, 93% and 94%, respectively. This effect is mainly due to a reduction in the number of functional α7 receptors reaching the oocyte membrane, as deduced from α-bungarotoxin binding and fluorescent confocal assays. Two additional findings open the possibility that the dominant-negative effect of dupα7 on α7 receptor activity observed *in vitro* could be extrapolated to *in vivo* situations: (i) compared with α7 mRNA, basal dupα7 mRNA levels are substantial in human cerebral cortex and higher in macrophages; and (ii) dupα7 mRNA levels in macrophages are down-regulated by IL-1β, LPS and nicotine. Thus, dupα7 could modulate α7 receptor-mediated synaptic transmission and cholinergic anti-inflammatory response.

Neuronal α7 nicotinic acetylcholine receptors (α7 nAChRs) are widely expressed in the central and peripheral nervous systems. In neurons, homomeric α7 nAChRs, composed of five α7 subunits, modulate neurotransmitter release in presynaptic nerve terminals and induce excitatory impulses in postsynaptic neurons (1-4). Signaling through α7 nAChRs in the central nervous system has been associated with neuronal plasticity and cell survival (5-7), while impaired activity of this receptor has been implicated in the pathogenesis of schizophrenia, Alzheimer´s disease and depression (8-12). The presence of α7 nAChRs has also been reported in non-neuronal cells such as vascular and brain endothelial cells, bronchial epithelial cells, keratinocytes, astrocytes, synoviocytes, thymocytes, lymphocytes, bone marrow cells,

monocytes, macrophages, microglia and astrocytes [see (13) and the references therein]. Interestingly, the α7 nAChR expressed in macrophages (and probably in other immune cells) is essential for vagus nerve regulation of acute pro-inflammatory cytokine release during systemic inflammatory response [see (14) and references therein]. The α7 nAChR is a target for natural and synthetic ligands; however, little is known about endogenous receptor-regulating molecules.

The α7 nicotinic subunit encoded by gene *CHRNA7* is located on the long arm of chromosome 15(15q13-q14). A hybrid gene (*CHRFAM7A)* resulting from a fusion of a partial duplication of *CHRNA7* with *FAM7A* gene was identified at 1.6 Mb from *CHRNA7* toward the centromeric region (15-16). *CHRNA7* and *CHRFAM7A* are highly homologous (> 99%) from exon 5 until the 3'-UTR region. In contrast, the hybrid has replaced exons 1-4 of the original *CHRNA7* with the exons D, C, B, A of *FAM7A*, inserted in an Alu sequence of intron 4 of *CHRNA7*, 700 bp upstream from exon 5. Moreover, *CHRFAM7A* is polymorphic with a few rare individuals who completely lack a copy of the gene. Most people (> 95%) have one or two *CHRFAM7A* copies and, in some cases, there is a 2 bp deletion in exon 6 (16-17). The acquisition of this duplication seems to be a recent evolutionary event since *CHRFAM7A* only appears in humans but not in other higher primates (18). The above findings would indicate that the hybrid gene could confer an evolutionary advantage on the genotype with the duplication.

To date, the possible functional significance of this *CHRNA7* duplication is unknown, although there are conflicting reports in the literature suggesting an association between *CHRFAM7A* polymorphisms and certain psychiatric and neurological disorders, such as schizophrenia, bipolar depression, Alzheimer´s disease, dementia with Lewy bodies or Pick's disease (19-24). The *CHRFAM7A* transcript, dupα7, has been identified in hippocampus, cortex, corpus callosum, thalamus, putamen, caudate nucleus and cerebellum (15, 25-26) and in peripheral blood mononuclear cells (PBMC), lymphocytes, synoviocytes as well as HL-60 cells (25-28). Despite its wide distribution, to date there are no experimental evidences demonstrating that this transcript is translated and what the possible functional role of the resulting protein might be.

This particular paper seeks to shed some light on the last two questions. Using GH4C1 cells and oocytes, we have studied the function of heterologously expressed dupα7 protein while, to study the native transcript, we use HL-60 cells, human CTX and human macrophages. A set of experimental approaches, including molecular biology and confocal images of labeled receptors, combined with pharmacological and electrophysiological techniques, have been used throughout this study.

Experimental Procedures

Cell Lines and Oocytes— The rat pituitary-derived GH4C1 cells were grown in DMEM containing 10% fetal calf serum, the human acute promyeloid leukemic HL-60 cell line in RPMI 1640 medium supplemented with 10% fetal bovine serum. In both cases, 100 units.ml^{-1} of penicillin G sodium and 100 μg·ml^{-1} of streptomycin sulfate were added. Both cell types were maintained at a density of 1x10^6 to 2x10^6 cells/ml at 37 ºC in a humidified 5% CO_2 atmosphere. Mature female *X. laevis* frogs were obtained from a commercial supplier (*Xenopus* Express, Haute-Loire, France). Techniques for oocyte isolation have been described by our group elsewhere (29-32).

Isolation of Human Monocytes and Differentiation to Macrophages — The PBMCs were isolated from blood buffy coats from healthy individual donors and then, the monocyte-enriched cell population was purified from PBMC by a double density-gradient protocol as previosly described (33). Monocytes were collected, washed, resuspended in complete RPMI 1640 medium and seeded either onto coverslips in 24-well tissue culture plates (5x10^5 cells per well) or onto 60 mm Petri dishes (10^6 cells·ml^{-1}). Cells were allowed to diferentiate to macrophages (MØ) for 7-9 days in the presence of macrophage colony stimulating factor (MCSF; 2 ng·ml^{-1}) in complete culture medium.

Cloning of dupα7 cDNA — Dupα7 was cloned in two steps, using either human thalamus (for the 3' region) or MØ (for the 5' region) RNAs. After first strand cDNA synthesis with

M-MLV reverse transcriptase (Gibco/BRL), the 3'-region was amplified with primers: A7S4 (5´-CACACACGTCTCGCCCTCGCCCTGCTG-GT-3´); and A7AS4 (5´-CACCCCCAAATCTC-GCCAA-3´). We amplified the 5'-region with primers: DUPA7S (5´-TGACAATCCA-AAGGTGCACA-3´) and A7AS3 (5´-CACACACGTCTCGAGGGCGGAGATGAG-CA-3´). Both fragments were cloned in pMOS-Blue. To obtain the whole coding sequence, the 3'-region fragment was digested with BsmBI (underlined in primers A7S4 and A7AS3) and SacI and ligated to the vector containing the 5'-region, digested with the same enzymes. The complete cDNA was transferred directly from dupα7·pMOS-Blue to pcDNA3 (digested with XbaI and BamHI). For oocyte injection experiments, dupα7 was amplified from dupα7·pMOS-Blue with DupSpeI(S) 5´-ACTAGTGCCACCATGCAAAAATATTGCA TCTACC-3´ and DupNotI(AS) 5´-GCGGCCGCCGTGGTTACGCAAAGTCTTTG G-3´ (with the recognition sequences for SpeI and NotI underlined, respectively) and cloned into pSP64T digested with the same enzymes.

Preparation of RNAs — Techniques for RNA isolation from cells and tissues and *in vitro* transcription mRNA synthesis have been described elsewhere (31-32). Plasmids dupα7·pSP64T, α7·pSP64T and RIC3·pGEMH19 were linearized with BamHI, Xba and NheI, respectively, and then *in vitro*-transcribed with SP6 (dupα7, α7) or T7 (RIC3) polymerases using the mMACHINE kit from AMBION (Austin, TX, USA). Messenger RNA was dissolved in RNAse-free water (1μg/μl) and aliquots stored at –80ºC until use.

Immunofluorescent Staining and Confocal Microscopy— GH4C1 cells were electroporated with plasmids dupα7·pcDNA3, α7·pcDNA3 or pcDNA3. Then, they were plated on 12-mm glass coverslips for 48 h before processing. Cells were fixed with 4% paraformaldehyde, permeabilized with 0.25% Triton X-100 and stained overnight with the monoclonal anti-α7 subunit antibody (Mab 306, Sigma-Aldrich, 1:3000) in PBS with 5% normal goat serum (NGS) at 4ºC, followed by incubation with AlexaFluor 488 goat anti-mouse IgG (1:400) for 2h at room temperature. All images were captured with a Leica TCS SP2 Spectral confocal laser scanning microscope as reported previously (31-32). Fluorescence intensity, expressed as arbitrary units (a.u.), was measured in a narrow region of interest (ROI) located between the plasma membrane and the cell nucleus. In other cases, fluorescence intensity was measured along the *X*-axis of the entire cell body.

Techniques for mRNA injection and immunodetection of foreign proteins expressed in intact injected oocytes have been described elsewhere (31-32). Five days after injection, protein expression was analyzed using the same antibodies and dilutions as for GH4C1 cells. Oocytes were mounted in glycerol/buffer (70:30) under a glass coverslip on a glass dual-well slide. The slide was fastened upside down on the stage of the Leica confocal microscope and visualized with a 20X lens. The fluorescent signal was determined as a.u. in an ROI located on the animal surface of the oocyte.

α-Bungarotoxin Staining and Confocal Microscopy — Native expression levels of functional α7 nAChRs in MØ were analyzed using fluorescein isothiocyanate-labeled α-bungarotoxin (FITC-αBgtx) and confocal microscopy. Cells were incubated with FITC-αBgtx ($3\,\mu g\cdot ml^{-1}$; Sigma) as previously described (34). Cells from the same culture incubated with nicotine (500 μM) or αBgtx(1 μM), before and during the addition of FITC-αBgtx, were used as a negative control. After several rinses, MØ were 4% paraformaldehyde-fixed, washed and mounted on coverslips. Heterologous expression of functional α7 nAChRs in mRNA-injected oocytes was analyzed 5 days after injection by incubation with FITC-αBgtx ($3\,\mu g\cdot ml^{-1}$) in Barth's solution, as has been described for MØ. Oocytes were rinsed, fixed in 4% paraformaldehyde, mounted in glycerol/buffer (70:30), and visualized by confocal microscopy. Fluorescent signal was determined as described elsewhere (31-32).

Electrophysiological Recordings and Surface Receptor Binding Assay — Electrophysiological recordings of foreign proteins expressed in oocytes have been described in detail by our group elsewhere (29, 32, 35). The agonist concentration eliciting half-maximal current (EC_{50}) and the Hill coefficient values were estimated through nonlinear regresion analysis using the four-parameter logistic equation of the

GraphPad Prism sofware. Total surface expression of αBgtx binding sites on the surface of mRNA-injected oocytes was assayed with [^{125}I]α-Bgtx (Amersham Pharmacia Biotech, Little Chalfont, UK), as described elsewhere (36). Briefly, five days after injection, oocytes placed on 24-well plates were preincubated during 15 min with Ringer's solution containing fetal calf serum (6%). Then they were incubated for 2 h at 18ºC in a final volume of 300 µl of the above solution containing increasing concentrations (1-10 nM) of [^{125}I]α-Bgtx. After incubation, labeled medium was removed and oocytes washed several times with Ringer's solution before counting total bound radioactivity in a Beckman Coulter γ counter. Nonspecific binding was determined in non-injected oocytes incubated under the same conditions; this value was subtracted from total binding to yield specific binding.

Northern Blot Analysis — Poly(A)$^+$ RNAs (4 µg/lane) isolated from human CTX and from HL-60 cells were separated by 1% formaldehyde/agarose gel electrophoresis, transferred onto a nylon blotting membrane (Schleicher & Schuell, Dassel, Germany) and hybridized at 68ºC overnight with the ^{32}P-labeled probe (781 bp) obtained by digestion of dupα7·pMOS-Blue with SpeI and SmaI. The resulting fragment starts in the ATG of exon B and extends to the 51 nucleotide of exon 10; thus, it recognizes the dupα7 and α7 transcripts.

Isolation of Polysome-Bound mRNA and Real-Time Quantitative PCR (Q-PCR) — Polysome-bound mRNA from HL-60 cells was obtained as described by Del Prete and coworkers (37), except that cells were pretreated with 0.1 mg·ml^{-1} cycloheximide for 10 min at 37ºC. In the conditions used, ribonucleoprotein particles, isolated ribosomal subunits and monosomes remain in fractions 1-10 (from the top) while polysomes are recovered in fractions 11-20. After this, monosomic and polysome fractions were regrouped into two pools and one aliquot (10 µl, diluted to 100 ng·µl^{-1}) from each pool was used for Q-PCR mRNA quantification. We added 10 ng of *in vitro* transcribed luciferase mRNA (from pGL3-control plasmid) to each aliquot as an endogenous marker for quantification . The level of gene expression in human CTX and human MØ was also assessed by Q-PCR for reverse transcribed mRNA or total RNA, respectively. A combination of Taq-Man and SYBR green-based assays for amplicon detection on the ABI Prism 7900 device was used. The following primers were used: for dupα7, forward 5´-CAATTGCTAAT-CCAGCATTTGT-3´ (position 603-624 of sequence in NM_139320) and reverse 5´-CC-CAGAAGAATTCACCAACACG-3´ (position 704-683 in NM_139320); for α7, Hs_CHRNA7_2_SG, Quantitec Primer Assay, QT01681211 (Qiagen); for TBP (encoding for the TATA binding protein), forward 5´-CGGTTTGCTGCGGTAATCA-3´ and reverse 5´-TGTTGGTGGGTGAGCACAAG-3´; for luciferase, forward 5´-TGGAAGA-CGCCAAAAACATAAAG-3´ and reverse 5´-AGCAATTGTTCCAGGAACCAGGGC-3´. For dupα7 and α7 mRNA quantification in MØ, TaqMan Hs00415199_m1 and Hs01063372_m1 (Applied Biosystems) were respectively used. Analysis of the melting curves demonstrated that each pair of primers amplified a single product. Q-PCR reaction for each mRNA was performed in triplicate and all results normalized to the expression of 18S rRNA (Ambion primers). Relative gene expression values were calculated by the comparative delta Ct method using the Sequence Detection System 1.2 software (Applied Biosystems).

Chemicals— Unless otherwise indicated, all products were purchased from SIGMA (Madrid, Spain). AlexaFluor 488 goat anti-mouse IgG was from Molecular Probes (Eugene, OR, USA) and DMEM and RPMI media from Gibco (Invitrogen, UK). The human recombinant IL-1β was purchased from Peprotech (London, UK) and PNU120596 from Tocris Bioscience (Bristol, UK).

RESULTS

Analysis of the dupα7 Coding Sequence— The cloned full-length dupα7 cDNA codes for a 1236 nucleotide sequence similar to the one previously deposited in NCBI and which corresponded to the dupα7 isoform 1 (accession number NM_139320), with minimal variations. Our sequence contains two neutral transitions: C/T and A/G at positions 654 and 986, respectively, but it retains the two TG nucleotides at positions 497-498 on exon 6. Using the ConPred II software for

transmembrane topology prediction, one can observe that the resulting 412 aa. polypeptide preserves many of the distinctive features of the nAChR subunits, with the N- and C-terminals outside the membrane and the four transmembrane domains (M1-M4) as well as the long intracellular loop between M3 and M4 (Fig. 2A). However, as has been reported previously (15), dupα7 protein does lose a substantial part of the long N-terminal domain of α7 and thus lacks the recognition sites for ACh and α-Bgtx.

Heterologous Expression of dupα7 versus α7— Expression of foreign proteins was analyzed in GH4C1 cells transfected with plasmids dupα7·pcDNA3 or α7·pcDNA3 and in oocytes injected with dupα7 and α7 mRNAs. The GH4C1 cell line was selected for two reasons: 1) it does not express dupα7 or α7, making visualization of foreign protein expression feasible; and 2) it expresses the RIC-3 chaperone (38) making it an excellent model to express functional α7 nAChRs. The confocal images obtained in transfected GH4C1 cells stained with Mab306 show a high expression level of both proteins, in contrast to low fluorescence detected in the negative control cells transfected with pcDNA3 (Fig. 1, A and C). The analysis of the protein expression along the *X* axis of the cell reveals two expression peaks located in the cell periphery; the α7 peak seems to be located more externally than the dupα7 peak (Fig. 1 B).

Non-injected oocytes (control) have low basal fluorescence, which increases markedly at or near the cell surface of the animal hemisphere in dupα7 or α7 mRNA-injected oocytes incubated with the above antibody (Fig. 2B). Nevertheless, the fluorescence signal corresponding to dupα7 is significantly lower (33 ± 7%, n = 7; $p \leq 0.05$) than that found in α7 mRNA-injected oocytes. As has been reported previously, no intracellular fluorescence was observed in mRNA-injected oocytes under any experimental condition (39). This may be due to: 1) the inability of the laser to penetrate far into a large 1 mm cell; 2) the quenching of the fluorescent signal by the oocyte yolk/pigment; or 3) the possibility that intracellular antibody distribution may be too diffuse to be detected.

Dominant Negative Effect of dupα7 on α7 Currents Expressed in Oocytes — Once the heterologous expression of the dupα7 protein in GH4C1 cells and oocytes was confirmed, we proceeded to study its possible functional role in the latter cell type. The study began with the electrophysiological recording of ACh-elicited currents [I_{ACh}] in oocytes injected with α7 mRNA (2.5 ng/oocyte). In all experiments RIC3 mRNA (2.5 ng) was co-injected with α7 mRNA since this treatment almost doubles the amplitude and reproducibility of the recorded currents. Repeated pulses of ACh (100 μM, 1s) or nicotine (30 μM, 1s) at 1 min intervals, applied to oocytes injected with increasing concentrations of dupα7 mRNA (from 0.5 to 25 ng/oocyte), failed to produce any response (not shown). In contrast, co-injection of dupα7 with α7 mRNA (2.5 ng) resulted in a concentration-dependent reduction of α7 current induced by nicotine, I_{Nic} (Fig. 3, A and B). The co-injection of 0.5 ng/oocyte of dupα7 mRNA (α7:dupα7 ratio of 5:1) was sufficient to reduce significantly (26 ± 8%, n= 6; $p \leq 0.01$) the amplitude of I_{Nic} and this blockade exceeded 90% when the α7:dupα7 ratio was 1:5 or 1:10.

The next experiments were designed to analyze the nature of the dominant negative effect of dupα7 on the α7 current. One possibility is that dupα7 is integrated into the pentameric structure of the expressed receptor, changing its pharmacological properties. Another possibility is that dupα7 interferes with the proper assembly of α7 subunits that form mature homopentameric α7 nAChR, which is essential for receptor trafficking from endoplasmic reticulum (ER) to the cell membrane. The following experiments sought to explore both possibilities.

Dupα7 Reduces α7 Current Amplitude but not Receptor Response to *ACh* — Figure 3 (C and D) shows the concentration-response curves to ACh in oocytes injected with 2.5 ng of α7 mRNA and the corresponding amount of dupα7 mRNA according to the indicated α7:dupα7 ratio. Each oocyte was stimulated with successive pulses of increasing concentrations of agonist and, at the end of experiment, with a control pulse of 1 mM ACh that induced the maximum current [I_{max}]. Figure 3C shows the original traces of I_{ACh} obtained in one α7 mRNA-injected oocyte stimulated as described above. As expected, for a given ACh

concentration, the higher the proportion of dupα7 in the mixture of injected mRNA, the lower the I_{ACh}. Thus, the I_{max} for the combinations 1:0, 2:1, 1:1 and 1:5 of α7: dupα7 was 8.4 ± 1.5 μA, 3.9 ± 0.7 μA, 2.1 ± 0.5 μA and 0.6 ± 0.2 μA, respectively. The currents induced by each of the ACh concentrations tested in the oocyte were normalized to the I_{max}. Figure 3D shows pooled results of normalized currents obtained in several oocytes (n = 5-6) assayed for each condition; each value represents mean ± SEM. The EC_{50} and Hill coefficient values are shown in the table below; the analysis of variance (ANOVA) applied to both parameters showed no significant differences between the four groups of oocytes.

Dup α7 Reduces the Number of Functional α7 nAChRs in the Oocyte Membrane— To examine whether the dupα7 effect was due to a reduction in the number of functional α7 nAChRs incorporated into the surface of the oocyte, we incubated the oocytes with either the Mab306 antibody, which detects both α7 and dupα7, or with FITC-αBgtx, which binds to the extracellular N-terminal region present in the α7 subunit alone. Three groups of mRNA-injected oocytes (α7, dupα7 or 1:1 α7:dupα7), along with a fourth group without an injection (control) were analyzed. The confocal images in Figure 4A show the fluorescent signal detected in eight typical intact oocytes from the same donor subjected to one or the other staining process. Figure 4B shows the average fluorescence values, expressed as a percentage of the control, determined in several oocytes (n = 5-8) used for testing each experimental condition. While the antibody detected a robust expression of α7 nAChRs and a small fluorescent signal generated by dupα7 in oocytes injected with one or the other mRNA, FITC-αBgtx only detected the expression of the first protein. However, regardless of the staining technique used, the co-injection of dupα7 with α7 mRNA significantly reduced the expression of α7 nAChRs on the surface of the oocyte. In fact, in oocytes labeled with FITC-αBgtx, the α7 signal was reduced (≈ 70%) to levels that were indistinguishable from those in the control. It should be noted that, regardless of the staining process used, confocal images show a polarized distribution of nicotinic subunits on the animal membrane of the oocyte.

Coexpression of dupα7 with α7 Reduces the Number of [^{125}I]α-Bgtx Binding Sites on the Oocyte Surface —Two groups of oocytes injected with α7 mRNA (control) or with the combination 1:4 of α7:dupα7 mRNA were incubated with increasing concentrations of [^{125}I]α-Bgtx as described in "Experimental Procedures". Compared to controls, the injection of dupα7 mRNA reduced markedly and significantly the maximum specific binding of radioligand (B_{max}), from 8,277±331 to 4,552± 288 cpm; $p \leq 0.01$ (Fig. 4C, bottom). Additionally, the equilibrium dissociation constant (Kd) suffered a slight but significant increase in the presence of dupα7 (from 1.37±0.17 to 4.28±0.56 nM; $p \leq 0.05$).

Effect of Positive Allosteric Modulators on I_{ACh} Expressed in Oocytes Injected with Several Combinations of α7:dupα7 mRNA—The following experiments were designed to look for possible pharmacological differences among oocytes injected with different α7:dupα7 mRNA ratios. We used two positive allosteric modulators (PAMs) of α7 nAChRs, each one representative of one of the two available allosteric groups. Group-I includes agents like 5-hydroxyindole (5HI), which potentiates the peak agonist-evoked response mediated by α7 nAChR, but it does not modify the duration of the response (40). Meanwhile, PNU120596, representative of Group-II, increases the peak agonist-evoked response and markedly prolongs the macroscopic currents in the presence of agonist, possibly by interfering with the desensitization process (41). The different effects of these two groups of PAMs indicate the existence of distinct allosteric binding sites with specificity for either 5HI or PNU120596.

The effects of 5HI on I_{ACh} were analyzed in several groups of oocytes injected with different combinations of α7: dupα7 mRNA, using the group of α7 mRNA-injected oocytes as reference (Fig. 5, upper left). The oocytes were stimulated with successive pulses of ACh (30 μM, 1s), applied at intervals of 1 min. Once the I_{ACh} was stable (control), we incubated the oocytes with 3 mM 5HI (30s before and during the ACh pulse), evaluating its enhancing effect on control I_{ACh}. Figure 5 (A, B) shows that 5HI increased the amplitude of control I_{ACh} about 5-fold and that this effect was not significantly different in any oocyte group. Additionally, 5HI

did not alter the kinetics of I_{ACh} in any of the oocyte groups as can be deduced after normalization of the original traces obtained in two oocytes injected with either α7 or α7:dupα7 (1:1) mRNAs (Fig. 5A, inset).

A different design was used to evaluate the effect of PNU120596 in oocytes injected with several combinations of α7:dupα7 mRNA (Fig. 5, top right). The α7 mRNA-injected group was used as reference. The oocytes were stimulated with successive pulses of ACh (30 μM, 1s, at 1 min intervals). Once I_{ACh} was stabilized (control), we perfused 300 nM PNU120596 before and during the ACh pulse, evaluating its enhancing effect on control I_{ACh}. Since there was a progressive positive effect of the modulator on I_{ACh} over successive ACh pulses, we evaluated this effect over six consecutive agonist pulses. Figure 5 (C, D) shows that the higher the proportion of dupα7 in the mixture of injected mRNA, the lower the enhancing effect of PNU120596 on peak I_{ACh}. Normalization of the currents (Fig. 5C, inset) shows that the allosteric modulator delays desensitization of I_{ACh} in all the oocyte groups, with no significant differences, probably because of the shortness of the ACh pulse.

Identification of the dupα7 Transcript in Cerebral Cortex and HL-60 Cells—Although the presence of the dupα7 transcript has been detected in different brain areas, immune cell types and the HL-60 cell line by PCR, the size of this mRNA is unknown. Northern blot analysis was performed with mRNAs extracted from human CTX and HL-60 cells since the latter cell type mainly expresses dupα7 and not α7 (25). Figure 6A shows a well-defined band of ≈ 3.9 kb in HL-60 cells, also present in CTX, the latter also containing bands of 5.8, 3.3, 2.1 and 1.4 kb.

Dupα7 mRNA is Translated in HL-60 Cells—Antibodies that specifically differentiate α7 and dupα7 are not available, so it is still impossible to demonstrate the existence of dupα7 protein *in vitro* or *in vivo*. To solve this difficulty we have gone a step backwards in the translation process and used an indirect approach, one that looks for dupα7 mRNA in the polysomal fraction since we know that polysome-bound mRNAs are being translated (42, 43). After sucrose gradient centrifugation of an HL-60 cell extract as described in "Experimental Procedures", a bioanalysis assay for each fraction showed that tRNA appears in fractions 1-4, the migration peak for the small 40S ribosomal subunit (18S peak) is in fractions 5-6, followed by the migration peak for the large 60S ribosomal subunit (28S peak) in fractions 7-10, while fractions 11-20 contain the polysomal fraction (28S and 18S). All fractions were regrouped into two pools (monosomal and polysomal) as described in "Experimental Procedures". Relative expression of dupα7, TBP and luciferase mRNAs was quantified in the two pools. TBP mRNA was used as the positive control since it is constitutively translated in all cell types and, therefore, must be present in the "polysomal fraction" of HL-60 cells. Figure 6B shows the relative levels of TBP mRNA and dupα7 mRNA in monosomal and polysomal pools, expressed as a percentage of the total mRNA in both fractions. The results reveal that, as expected, the TBP transcript was in the heavy sucrose fractions (polysomes), as was the dupα7 transcript.

Levels of the dupα7 Transcript in Human Cerebral Cortex and Macrophages and its Modulation by Different Treatments —We performed Q-PCR experiments to determine levels of dupα7 and α7 mRNAs in CTX and MØ. The PCR reaction was performed with human CTX mRNA or with total RNA from cultured human MØ using the primers listed in "Experimental Procedures". The results in Figure 7A show that dupα7 expression is around 22% of the α7 expression in CTX. The opposite happens in MØ, where the α7 mRNA levels are approximately 7% of those of dupα7. Despite this low level of α7 mRNA in relation to dupα7 in MØ, these cells clearly show the expression of functional α7 nAChRs, as reflected by confocal images of MØ in FITC-αBgtx labeled cultures (Fig. 7B, left). The receptor specificity of this staining is demonstrated by the disappearance of the fluorescent signal in cells preincubated with 1μM αBgtx or 500 μM nicotine (Fig. 7B, right). Finally, MØ in culture were subjected to different treatments to evaluate if dupα7 mRNA levels could be modulated. Figure 7C shows that the pro-inflammatory cytokine interleukin-1β (IL-1β), LPS from Salmonella abortus and nicotine, all markedly and significantly reduced dupα7 mRNA expression in MØ cultures (Fig. 7C).

DISCUSSION

In this study we have cloned and expressed, for the first time, the full-length coding sequence of dupα7 in GH4C1 cells and oocytes. Additionally, we have performed a functional study of the protein expressed in the latter cell type. Our results indicate that dupα7 acted as a dominant negative regulator of α7 nAChR activity through a mechanism involving reduction in the number of functional α7 nAChRs incorporated into the oocyte surface. Determining whether the dupα7 subunit plays a functional role *in vivo*, wherever it is co-expressed with α7, requires additional experiments but our preliminary results obtained in human cerebral cortex, human macrophages and HL-60 cells suggest this possibility. Here we discuss the most relevant results of the present study.

The parallel confocal analysis of dupα7 and α7 protein expression in transfected GH4C1 cells and in mRNA-injected oocytes labeled with the Mab306 antibody indicates that the two cell types express both foreign proteins, although their patterns and expression levels differ. Thus, GH4C1 cells show a similar high α7 and dupα7 expression (Fig. 1, A and C), although a careful analysis of the α7 expression along the *X* axis of the cell reveals a peak localized in the cell membrane while the dupα7 expression peak seems to have an inner location, probably within the ER (Fig. 1B). Meanwhile, expression levels of dupα7 on the cell surface of mRNA-injected oocytes represent only one third of that of the α7 subunit (Fig. 2B), making it likely that most of the synthesized dupα7 proteins in oocytes are retained in the ER. However, our data do not preclude the possibility that a small fraction of dupα7 can form homo- or heteropentameric structures with other nAChR subunits able to migrate to the cell membrane.

Despite the low expression of dupα7 compared to α7 in the oocyte surface, there is no doubt that the first protein clearly interferes with the second. This assertion is deduced from electrophysiological records of I_{Nic} obtained in oocytes injected with different combinations of α7:dupα7 mRNA (Fig. 3, A and B). Thus, although dupα7 subunits are not capable of forming, by themselves, homomeric nAChRs activated by ACh or nicotine (not shown), they do produce a concentration-dependent dominant negative regulatory effect on α7 current. The question that now arises is to identify the mechanism through which dupα7 exerts this effect. The following hypotheses, individually or in combination, could provide an answer. Thus, dupα7 could: 1) act at the transcriptional level of *CHRNA7*; 2) interfere with the proper oligomerization and assembly of α7 subunits in the ER, decreasing the number of mature α7 nAChRs able to migrate to the oocyte membrane; and/or 3) be integrated into a putative "α7/dupα7 heteromeric receptor" whose affinity or gating mechanism would be affected by the incorporation of the atypical subunit.

The first proposal can be ruled out, at least in terms of the dominant negative effect of dupα7 on α7 nAChRs in oocytes because, in this case, the injected mRNAs are obtained by *in vitro* transcription from the corresponding cDNAs. Although our results cannot rule out the possibility that dupα7 might produce some kind of interference *in vivo* at the transcriptional level of *CHRNA7*, this is unlikely since native transcripts that effectively regulate gene expression are "antisense" (44) and the orientation of the dupα7 transcript in human brain is in the "sense" direction of transcription (26).

Collectively, our data tend to support the second hypothesis since dupα7 coexpression significantly reduces the number of α7 nAChRs expressed on the oocyte surface, as can be inferred by the drastic decrease of fluorescent signal in Mab306-incubated oocytes as well as by the reduction of the B_{max} in [^{125}I]α-Bgtx binding assays (Fig. 4). This hypothesis is further reinforced by the similar degree of reduction of both I_{Nic} (≈ 74%) and α7 nAChR expression (≈ 70%) in FITC-αBgtx labeled oocytes injected with equimolar amount of α7 and dupα7 mRNAs (Figs. 3B and 4B-right).

In relation to the third hypothesis, two of our findings seem to support this alternative in combination with the second proposal raised above. On the one hand, there was a small but statistically significant increase of Kd in oocytes co-injected with the combination 1:4 of α7:dupα7 mRNA compared to those injected

with α7 mRNA alone (Figure 4C, bottom). Since Kd is the reciprocal of affinity, the higher the Kd, the lower the affinity of the receptor expressed by Bgtx. On the other hand, there was a different behavior of PNU120596 and 5HI in relation to their ability to enhance I_{ACh} in oocytes injected with different combinations of α7:dupα7 mRNA (Fig. 5). While the former drug distinguishes between different groups of oocytes, the second does not. These results can be interpreted in light of different α7 modulation sites required by one or the other PAM, because PNU120596 interacts with transmembrane domains while 5HI requires the extracellular N-terminal domain of the α7 subunit (40, 45, 46). Thus, PNU120596 could act on homo- and heteromeric receptors, while 5HI would do so only on homomeric α7 nAChRs.

Northern blot analysis shows a band of a size of 3.9 kb in human CTX and HL-60 cells that most likely corresponds to the dupα7 transcript (Fig. 6A). This assumption is based on two facts: 1) the HL-60 cells appear to express only dupα7 transcript (25); and 2) analysis of the NCBI EST database provides a theoretical prediction of the size of dupα7 mRNA of 3,600 bp. If we added the about 200 bp corresponding to the poly(A^+) tail to this value, there is a good correlation between the predicted and the experimental size of dupα7 mRNA found in the present study. The possibility that the 3.9 kb band of CTX corresponds to an α7 isoform is very remote because we have not been able to find any isoform with this size in the literature or in NCBI EST database. In fact, the northern blot for the CTX mRNA in our study shows additional bands which probably correspond to several α7 isoforms since their sizes are consistent with those found in SHY-5Y cells (47, 48). Additionally, GeneBank sequence NM_000746 gives a size of the transcript encoded by the *CHRNA7* gene of 3,351 bp, which could correspond to the band of 3.3 kb identified in our experiments. By identification of polysome-bound mRNAs, our results show, for the first time, that dupα7 mRNA is being translated in HL-60 cells (Fig. 6B), a process that has not been demonstrated before because of the unavailability of a selective antibody.

After demonstrating that dupα7 mRNA is translated and that the resulting protein behaves as a dominant negative of α7 nAChR activity in *vitro*, it is time to consider whether dupα7 could play a relevant functional role *in vivo* in those tissues and cell types that also express α7 nAChRs, such as the central nervous system (49-51) where presynaptic α7 nAChRs regulate the release of different neurotransmitters (1-4, 52). The same can be said of α7 nAChRs in MØ, which have an essential role in the cholinergic anti-inflammatory response (34, 53-56). However, to assume that dupα7 could behave as an endogenous modulator for α7 nAChR activity *in vivo*, it is essential that it meet two conditions: (i) its mRNA levels must be high enough in respect to α7 and/or (ii) the expression levels of this messenger should, in turn, be susceptible to modulation by external stimuli that require greater or lesser α7 activity.

When we explored the first condition in human CTX and MØ using Q-PCR we found that dupα7 mRNA levels in the former tissue come to about one-fifth of those of α7 (Fig. 7A). This result is consistent with previous data obtained in human prefrontal cortex showing that expression of α7 mRNA is five times higher than that of dupα7 (21). The low proportion of dupα7 relative to that of α7 mRNA in CTX is functionally relevant in accordance with our data from I_{Nic} recorded in oocytes injected with the combination 5:1 of α7:dupα7 mRNA (Fig. 3, A and B).

A result opposite to that of CTX was obtained in MØ, which preferentially express dupα7 over the α7 transcript (Fig. 7A). Human PBMC and lymphocytes (25, 27, 57), and HL-60 cells (Fig. 6A) behave similarly. Despite the low expression level of α7 mRNA in MØ, there is no doubt that it is efficiently translated given the high number of functional α7 nAChRs detected in our experiments (Fig. 7B) as well as in previous studies (34). Thus, the question now is why, despite the high level of dupα7 mRNA in MØ, α7 nAChR expression is high in these cells. At this time we do not have a convincing answer, although different efficiencies in translation and/or proper folding of the α7 and dupα7 proteins could be underlying these results. Additional experiments are needed to explore these possibilities.

In relation to the second condition for dupα7's playing a modulatory role *in vivo*, our results in MØ show that mRNA levels are

actually being regulated (Fig. 7C). This is an interesting finding since stimulation of α7 nAChR in macrophages induces a clear anti-inflammatory response secondary to decreased production of pro-inflammatory cytokines (34, 53, 56, 58). In this context, our results show that one of these cytokines, IL-1β, as well as LPS, is able to reduce dupα7 mRNA expression by half. In these conditions, pro-inflammatory cytokines would repress dupα7 expression, and therefore increase the number of functional α7 nAChRs; the net output of this feedback loop would be the attenuation of the inflammatory response. Additionally, our finding that nicotine markedly reduces the expression levels of dupα7 mRNA in MØ (Fig. 7C) are in complete agreement with recent *in vivo* results showing a lower α7 transcript expression in PBMC from smokers than from nonsmokers (57). Further experiments are needed to learn whether cerebral dupα7 mRNA expression can be regulated by different stimuli, as occurs in MØ. However, it is interesting to note that the ratio of the α7/dupα7 transcripts varies in different brain regions as well as in individuals addicted to drugs or suffering certain psychiatric disorders. This is the case in schizophrenic patients, who show a general decrease in brain α7 mRNA and all *CHRNA7* transcription products that is most marked in the corpus callosum (26). The effect of nicotine in reducing dupα7 mRNA levels found in our study could explain, at least in part, the relief of symptoms experienced by these patients after smoking. Also, in bipolar disorder, an imbalance in the ratio of *CHRNA7*/*CHRFAM7A* transcripts due to increased expression of dupα7 mRNA has been found (21).

In summary, our data are consistent with the idea that the product resulting from the partial duplication of the *CHRNA7* gene is likely to be modulated in a paracrine and endocrine manner, both in physiological as well as pathological situations, thereby exerting a negative modulating effect on α7 nAChR activity. Thus, previous findings regarding the *CHRFAM7A* and its possible association with psychiatric disorders can now be interpreted in the light of these new results.

REFERENCES

1. Li, D.P., Pan, Y.Z., and Pan. H.L. (2001) *Brain Res* 920, 151-158
2. Gray, R., Rajan, A.S., Radcliffe, K.A., Yakehiro, M., and Dani, J.A. (1996) *Nature* **383**, 713-716
3. Zhang, J., and Berg, D.K.(2007) *J Physiol* **579**, 753-763
4. Dickinson, J.A., Kew, J.N., and Wonnacott, S. (2008) *Mol Pharmacol* **74**, 348-359
5. Dajas-Bailador, F.A., Lima, P.A., and Wonnacott, S. (2000) *Neuropharmacology* **39**, 2799-2807
6. Mechawar, N., Saghatelyan, A., Grailhe, R., Scoriels, L., Gheusi, G., Gabellec, M. M., Lledo, P. M., and Changeux, J. P. (2004) *Proc Natl Acad Sci U S A* **101**, 9822-9826
7. Shaw, S., Bencherif, M., and Marrero, M.B. (2002) *J Biol Chem* **277**, 44920-44924
8. Freedman, R., Hall, M., Adler, L.E., and Leonard, S. (1995) *Biol Psychiatry* **38**, 22-33
9. Guan, Z.Z., Zhang, X., Blennow, K., and Nordberg, A. (1999) *Neuroreport* **10**, 1779-1782
10. Dineley, K.T., Westerman, M., Bui, D., Bell, K., Ashe, K.H., and Sweatt, J.D. (2001) *J Neurosci* **21**, 4125-4133
11. Oddo, S., and LaFerla, F.M. (2006) *J Physiol Paris* **99**, 172-179
12. Shytle, R.D., Silver, A.A., Lukas, R.J., Newman, M.B., Sheehan, D.V., and Sanberg, P.R. (2002) *Mol Psychiatry* **7**, 525-535
13. Arias, H.R., Richards, V.E., Ng, D., Ghafoori, M.E., Le, V., and Mousa, S.A. (2009) *Int J Biochem Cell Biol* **41**, 1441-1451
14. Rosas-Ballina, M., and Tracey, K.J. (2009) *Neuron* **64**, 28-32
15. Gault, J., Robinson, M., Berger, R., Drebing, C., Logel, J., Hopkins, J., Moore, T., Jacobs, S., Meriwether, J., Choi, M. J., Kim, E. J., Walton, K., Buiting, K., Davis, A., Breese, C., Freedman, R., and Leonard, S. (1998) *Genomics* **52**, 173-185

16. Riley, B., Williamson, M., Collier, D., Wilkie, H., and Makoff, A. (2002) *Genomics* **79**, 197-209
17. Gault, J., Hopkins, J., Berger, R., Drebing, C., Logel, J., Walton, C., Short, M., Vianzon, R., Olincy, A., Ross, R. G., Adler, L. E., Freedman, R., and Leonard, S. (2003) *Am J Med Genet B Neuropsychiatr Genet* **123B**, 39-49
18. Locke, D.P., Archidiacono, N., Misceo, D., Cardone, M.F., Deschamps, S., Roe, B., Rocchi, M., and Eichler, E. E. (2003) *Genome Biol* **4**, R50
19. Raux, G., Bonnet-Brilhault, F., Louchart, S., Houy, E., Gantier, R., Levillain, D., Allio, G., Haouzir, S., Petit, M., Martinez, M., Frebourg, T., Thibaut, F., and Campion, D. (2002) *Mol Psychiatry* **7**, 1006-1011
20. Hong, C.J., Lai, I.C., Liou, L.L., and Tsai, S.J. (2004) *Neurosci Lett* **355**, 69-72
21. De Luca, V., Likhodi, O., Van Tol, H.H., Kennedy, J.L., and Wong, A.H. (2006) *Acta Psychiatr Scand* **114**, 211-215
22. Flomen, R.H., Collier, D.A., Osborne, S., Munro, J., Breen, G., St Clair, D., and Makoff, A. J. (2006) *Am J Med Genet B Neuropsychiatr Genet* **141B**, 571-575
23. Feher, A., Juhasz, A., Rimanoczy, A., Csibri, E., Kalman, J., and Janka, Z. (2009) *Dement Geriatr Cogn Disord* **28**, 56-62
24. Sinkus, M.L., Lee, M.J., Gault, J., Logel, J., Short, M., Freedman, R., Christian, S. L., Lyon, J., and Leonard, S. (2009) *Brain Res* **1291**, 1-11
25. Villiger, Y., Szanto, I., Jaconi, S., Blanchet, C., Buisson, B., Krause, K. H., Bertrand, D., and Romand, J. A. (2002) *J Neuroimmunol* **126**, 86-98
26. Severance, E.G. and Yolken, R.H. (2008) *Genes Brain Behav* **7**, 37-45
27. Perl, O., Strous, R.D., Dranikov, A., Chen, R., and Fuchs, S. (2006) *Neuropsychobiology* **53**, 88-93
28. van Maanen, M.A., Stoof, S.P., van der Zanden, E.P, de Jonge, W.J., Janssen, R.A., Fischer, D. F., Vandeghinste, N., Brys, R., Vervoordeldonk, M. J., and Tak, P. P. (2009) *Arthritis Rheum* **60**, 1272-1281
29. Herrero, C.J., Garcia-Palomero, E., Pintado, A.J., Garcia, A.G., and Montiel, C. (1999) *Br J Pharmacol* **127**, 1375-1387
30. Pintado, A.J., Herrero, C.J., Garcia, A.G., and Montiel, C. (2000) *Br J Pharmacol* **130**, 1893-1902
31. Solis-Garrido, L.M., Pintado, A.J., Andres-Mateos, E., Figueroa, M., Matute, C., and Montiel, C. (2004) *J Biol Chem* **279**, 52414-524249
32. Serantes, R., Arnalich, F., Figueroa, M., Salinas, M., Andres-Mateos, E., Codoceo, R., Renart, J., Matute, C., Cavada, C., Cuadrado, A., and Montiel, C. (2006). *J Biol Chem* **281**, 14632-14643
33. de Almeida, M.C., Silva, A.C., Barral, A., and Barral Netto, M. (2000) *Mem Inst Oswaldo Cruz* **95**, 221-223
34. Wang, H., Yu, M., Ochani, M., Amella, C.A., Tanovic, M., Susarla, S., Li, J. H., Yang, H., Ulloa, L., Al-Abed, Y., Czura, C. J., and Tracey, K. J. (2003). *Nature* **421**, 384-388
35. Herrero, C.J., Ales, E., Pintado, A.J., Lopez, M.G., Garcia-Palomero, E., Mahata, S. K., O'Connor, D. T., Garcia, A. G., and Montiel, C. 2002. *J Neurosci* **22**, 377-388
36. Garcia-Guzman, M., Sala, F., Sala, S., Campos-Caro, A., Criado, M. (1994) *Biochemistry* **33**, 15198-15203
37. del Prete, M.J., Vernal, R., Dolznig, H., Mullner, E.W., and Garcia-Sanz, J.A. (2007) *RNA* **13**, 414-421
38. Sweileh, W., Wenberg, K., Xu, J., Forsayeth, J., Hardy, S., and Loring, R.H. (2000) *Brain Res Mol Brain Res* **75**, 293-302
39. Balduzzi, R., Cupello, A., Diaspro, A., Ramoino, P., and Robello, M. (2001) *Biochim Biophys Acta* **1539**, 93-100
40. Zwart, R., De Filippi, G., Broad, L.M., McPhie, G.I., Pearson, K.H., Baldwinson, T., and Sher, E. (2002) *Neuropharmacology* **43**, 374-384
41. Gronlien, J.H., Hakerud, M., Ween, H., Thorin-Hagene, K., Briggs, C.A., Gopalakrishnan, M., and Malysz, J. (2007) *Mol Pharmacol* **72**, 715-724
42. Pradet-Balade, B., Boulme, F., Beug, H., Mullner, E.W., and Garcia-Sanz, J.A. (2001) *Trends Biochem Sci* **26**, 225-229

43. Pradet-Balade, B., Boulme, F., Mullner, E.W., and Garcia-Sanz, J.A. (2001) *Biotechniques* **30**, 1352-1357
44. Osato, N., Suzuki, Y., Ikeo, K., and Gojobori, T. (2007) *Genetics* **176**, 1299-1306
45. Young, G.T., Zwart, R., Walker, A.S., Sher, E., and Millar, N.S. (2008) *Proc Natl Acad Sci U S A* **105**, 14686-14691
46. Bertrand, D., Bertrand, S., Cassar, S., Gubbins, E., Li, J., and , M. (2008) *Mol Pharmacol* **74**, 1407-1416
47. Peng, X., Katz, M., Gerzanich, V., Anand, R., and Lindstrom, J. (1994) *Mol Pharmacol* **45**, 546-554
48. Groot Kormelink, P.J., and Luyten, W.H. (1997) *FEBS Lett* **400**, 309-314
49. Chen, D., and Patrick, J.W. (1997) *J Biol Chem* **272**, 24024-24029
50. Court, J.A., Martin-Ruiz, C., Graham, A., and Perry, E. (2000) *J Chem Neuroanat* **20**, 281-298
51. Drisdel, R.C., and Green, W.N. (2000) *J Neurosci* **20**, 133-139
52. Sharma, G., and Vijayaraghavan, S. (2008) *Curr Med Chem* **15**, 2921-2932
53. Borovikova, L.V., Ivanova, S., Zhang, M., Yang, H., Botchkina, G.I., Watkins, L. R., Wang, H., Abumrad, N., Eaton, J. W., and Tracey, K. J. (2000) *Nature* **405**, 458-462
54. de Jonge, W.J., van der Zanden, E.P., The, F.O., Bijlsma, M.F., van Westerloo, D.J., Bennink, R. J., Berthoud, H. R., Uematsu, S., Akira, S., van den Wijngaard, R. M., and Boeckxstaens, G. E. (2005) *Nat Immunol* **6**, 844-851
55. Pavlov, V.A., and Tracey, K.J. (2006) *Biochem Soc Trans* **34**, 1037-1040
56. van Westerloo, D.J., Giebelen, I.A., Florquin, S., Bruno, M.J., Larosa, G.J., Ulloa, L., Tracey, K. J., and van der Poll, T. (2006) *Gastroenterology* **130**, 1822-1830
57. Severance, E.G., Dickerson, F.B., Stallings, C.R., Origoni, A.E., Sullens, A., Monson, E. T., and Yolken, R. H. (2009) *J Neural Transm* **116**, 213-220
58. Wang, H., Liao, H., Ochani, M., Justiniani, M., Lin, X., Yang, L., Al-Abed, Y., Metz, C., Miller, E. J., Tracey, K. J., and Ulloa, L. (2004) *Nat Med* **10**, 1216-1221

FOOTNOTES

***** This work was supported by grants to C. Montiel and F. Arnalich from the Ministerio de Ciencia y Tecnología (SAF2008-05347) and Fundación Mutua Madrileña, Spain. We thank Prof. Henk Sipma (J&J PRD, Division of Janssen Pharmaceutica N.V, Beerse, Belgium) for donating the plasmids α7·pST64 and α7·pCDNA.3 and Prof. Millet Treining (Medical School, The Hebrew University of Jerusalem) for providing the plasmid hRIC3·pGEMH19. We also thank the Transfusion Center of the Comunidad de Madrid for providing the human buffy coats. Our sincere gratitude to Prof. J. Javier Sanchez (Dept. of Preventive Medicine and Public Health, Medical School, UAM) for his advice in conducting statistical analysis. A.M. de Lucas and M.C. Maldifassi are recipients of fellowships from FPI (Ministerio de Ciencia y Tecnología, Spain), and Beca Chile (CONICYT, Ministerio de Educación, Chile), respectively.

The abbreviations used are: aa., amino acid; ACh, acetylcholine; αBgtx, alfa-bungarotoxin; a.u., arbitrary units; CTX, cerebral cortex; EC_{50}, agonist concentration eliciting half-maximal current; ER, endoplasmic reticulum; 5HI, 5-hydroxyindole; I_{ACh}, ACh-elicited current; I_{Nic}, nicotine-elicited current; Kd, equilibrium dissociation constant; MCSF, macrophage colony stimulating factor; MØ, macrophages differentiated from monocytes; nAChRs, neuronal nicotinic acetylcholine receptors; PAM, positive allosteric modulators; PBMCs; peripheral blood mononuclear cells; ROI, region of interest; Q-PCR, real-time quantitative PCR; TBP, TATA binding protein.

FIGURE LEGENDS

FIG. 1. **Expression of dupα7 and α7 subunits in GH4C1 cells. *A,*** Confocal images showing the fluorescent signal generated in transfected GH4C1 cells stained with the Mab 306 antibody. ***B,*** Scanned fluorescence intensity along the *X*-axis in three typical cells of the images above. ***C***, The histogram shows pooled results of fluorescence intensity measured in the region of interest (ROI) indicated in *B*. Each bar represents the mean ± SEM, expressed as a percentage of control (transfected with pcDNA3), in the number of cells shown at the top. At least four to six different coverslips from two independent cell cultures were used for each experimental condition. Data were analyzed using ANOVA and Bonferroni post-hoc tests, where ***p ≤ 0.001 upon comparing transfected *versus* control cells.

FIG. 2. **Confocal images of oocytes expressing dupα7 and α7 subunits. *A,*** Diagram of tertiary structures of α7 and dupα7 proteins; the Mab 306 antibody binding region is also indicated. ***B,*** Left column shows overall confocal (Z-scan) images of three typical intact oocytes (out of 5), non-injected (control) or injected with dupα7 or α7 mRNA and immunostained with the antibody. Central and right columns show, at a higher magnification, the fluorescent signal at the animal surface in the three oocytes.

FIG. 3. **Dupα7 produces a dominant negative effect on α7 currents without affecting receptor response to ACh.** In all combinations assaying α7:dupα7 mRNAs, the amount of injected α7 mRNA (2.5 ng/oocyte) remained constant. ***A***, Original traces of inward nicotine-elicited currents (I_{Nic}) in six oocytes injected with different combinations of α7:dupα7 mRNAs. Each oocyte was voltage-clamped at -70 mV and stimulated with repeated pulses of nicotine; the original traces correspond to the time when I_{Nic} becomes stabilized. ***B***, Diagram showing the I_{Nic} amplitude values for each α7:dupα7 combination normalized to α7 mRNA-injected oocytes. Each bar shows the mean ± SEM of the number of oocytes in parentheses. The data were analyzed using ANOVA and Dunnett post-hoc tests to compare all groups with the α7-mRNA injected group; **p ≤ 0.01 and ***p ≤ 0.001. ***C***, Original traces of inward currents (I_{ACh}) induced by increasing concentrations of ACh applied as succesive pulses in one α7 mRNA-injected oocyte; finally, a control pulse of 1 mM ACh to generate a maximum current (I_{max}) was applied. ***D***, Dependence of I_{ACh} amplitude, normalized to I_{max}, on the concentation of ACh assayed in oocytes injected with different combinations of α7:dupα7 mRNAs; values are mean ± SEM of the number of oocytes shown in parentheses in the table below. The table also shows mean ± SEM of EC_{50} and Hill coefficient values obtained for each combination tested. ANOVA analysis showed no significant differences among the four groups of oocytes analyzed.

FIG. 4. **Dupα7 reduces the number of functional α7 nAChRs expressed on the oocyte surface. *A,*** Representative confocal images of eight intact oocytes labeled with Mab 306 antibody (top row) or FITC-αBgtx (bottom row). Oocytes were injected with α7 (20 ng), dupα7 (20 ng), or with the combination (1:1) of α7:dupα7 mRNAs; on the left, two control non-injected oocytes. (*Inset*) Oocyte orientation on the confocal microscope stage; **V** and **A** indicate the vegetal and animal hemisphere, respectively. ***B,*** Histograms show pooled results of fluorescent intensity determined in an ROI located on the animal surface of the oocyte; data were normalized in respect to control. Each bar shows the mean ± SEM of the number of oocytes in parentheses. The data were analyzed by ANOVA, where *p ≤ 0.05, **p ≤ 0.01 and ***p ≤ 0.001 upon comparing injected with control oocytes. #p ≤ 0.05, ###p ≤ 0.001 after comparing oocytes injected with dupα7 or α7:dupα7 mRNAs *versus* α7-mRNA injected oocytes. ***C,*** Saturation curves showing specific binding of [^{125}I]α-Bgtx to the surface of intact oocytes injected with α7 mRNA (20 ng) or with the combination α7:dupα7 (20:80 ng). The adjustment of the curves and the determination of Kd and B_{max} values was done with GraphPad Prism5 sofware. The

analysis of the variation in Kd and B_{max} between the two groups of oocytes was performed with the Mann Whitney test for analysis of two non-parametric variables, * $p \leq 0.05$, ** $p \leq 0.01$. A total of 6-8 oocytes from two different donors were used for each value plotted in the curves.

FIG. 5. **The positive allosteric modulator PNU120596, but not 5-hydroxyindole, can distinguish among oocytes injected with different combinations of α7:dupα7 mRNAs.** The tested combinations and the experimental design are shown at the top. The α7 mRNA (2.5 ng/oocyte) remains constant in all combinations. Oocytes, voltage-clamped at -70 mV, were stimulated with regular pulses of ACh in the absence or presence of the modulator. The effect of 5-hydroxyindole (5HI) was evaluated on a single ACh pulse, while in the case of PNU120596 (PNU), the oocyte was stimulated with an initial pulse of ACh (0 = control) followed by six successive ACh pulses in the presence of the modulator. ***A,*** Original traces of ACh-elicited currents (I_{ACh}), in the absence or presence of 5HI, obtained in two mRNA-injected oocytes. The left and right records correspond to one α7-mRNA and one α7:dupα7-mRNA (1:1) injected oocyte, respectively. (*Inset*) Normalized currents of both oocytes. ***B,*** Histogram shows the number of times that 5HI increases the control peak I_{ACh} in each group of oocytes. Each bar shows the mean ± SEM of the number of oocytes in parentheses. ANOVA analysis and Dunnett post-hoc tests showed no differences between groups of oocytes. ***C,*** Original traces showing the PNU effect on I_{ACh} over the 1st to 6th pulses of ACh in two mRNA-injected oocytes. The left and right records correspond to one α7-mRNA and one α7:dupα7-mRNA (1:1) injected oocyte, respectively. (*Inset*) Normalized currents obtained in both oocytes corresponding to the initial (control) and the 3rd pulse of ACh in the presence of PNU. ***D,*** Graph representing the number of times that PNU increased the control peak I_{ACh} during the six pulses in each group of oocytes. Each point represents the mean ± SEM of 7 oocytes per group. Data were analyzed using ANOVA and Bonferroni post-hoc tests, where **$p \leq 0.01$, ***$p \leq 0.001$ and ## $p \leq 0.01$ after the comparison of the different oocyte groups as indicated.

FIG. 6**. Determination of the size and relative expression levels of dupα7 mRNA in the monosomal and polysomal fractions of HL-60 cells. *A,*** Northern blot performed with RNAs from human cerebral cortex (CTX) and HL-60 cells showing the 3.9 kb transcript in both lanes and different α7 transcript of 5.8, 3.3, 2.1 and 1.4 kb in CTX. ***B,*** Levels of dupα7 or TBP mRNAs in monosomal and polysomal fractions of HL-60 cells quantified by Q-PCR. The results are expressed as a percentage of each messenger in the two fractions. Values were obtained in triplicate and correspond to two different cultures of HL-60 cells subjected to ultracentrifugation on a sucrose gradient as described in *"Experimental Procedures"*.

FIG. 7. **Levels of dupα7 and α7 mRNA in different samples and regulation of dupα7 mRNA levels by different treatments. *A,*** Relative expression levels of dupα7 *versus* α7 mRNA in CTX and MØ determined by Q-PCR; values were obtained in triplicate and correspond to a single CTX sample and two cultures of MØ from different donors. ***B,*** Confocal images of MØ (out of 5) in culture immunostained with FITC-αBgtx (left). Cells from the same culture preincubated with a high concentration (500 μM) of nicotine (right). ***C,*** Effect of different treatments on the expression levels of dupα7 mRNA in cultured human MØ. Cells were incubated overnight with IL-1β (25 $ng \cdot ml^{-1}$), LPS (100 $ng \cdot ml^{-1}$) and nicotine (1 μM) or untreated. The bars show the mean ± SEM of values, obtained in triplicate, and quantified by Q-PCR in the number of cultures from different healthy donors shown in parentheses. Data were analyzed by ANOVA and Dunnett post-hoc tests; **$p \leq 0.01$ with respect to control.

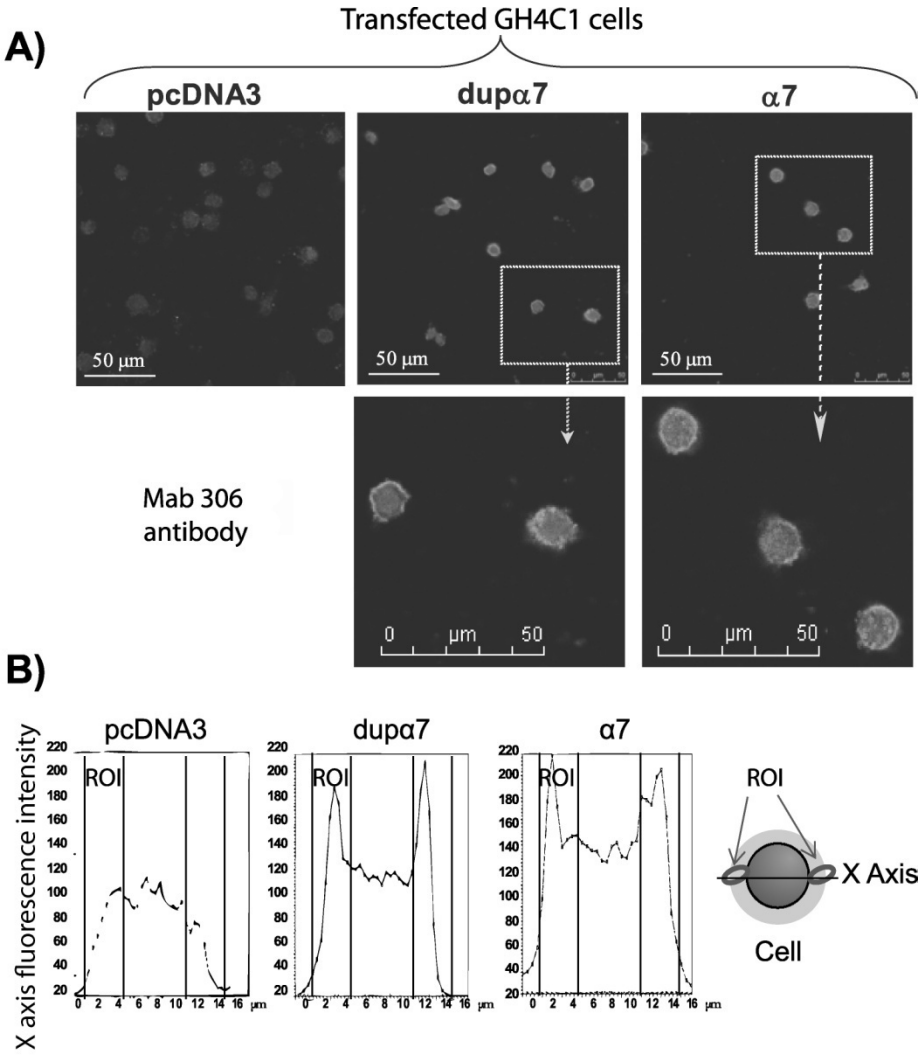
A)
Transfected GH4C1 cells
pcDNA3
dupα7
α7
50 µm
Mab 306
antibody
0 µm 50
B)
pcDNA3
dupα7
α7
ROI
X axis fluorescence intensity
X Axis
Cell
C)
Fluorescence intensity (% control)
44
30
52
***
pcDNA3
α7
dupα7

Figure 1

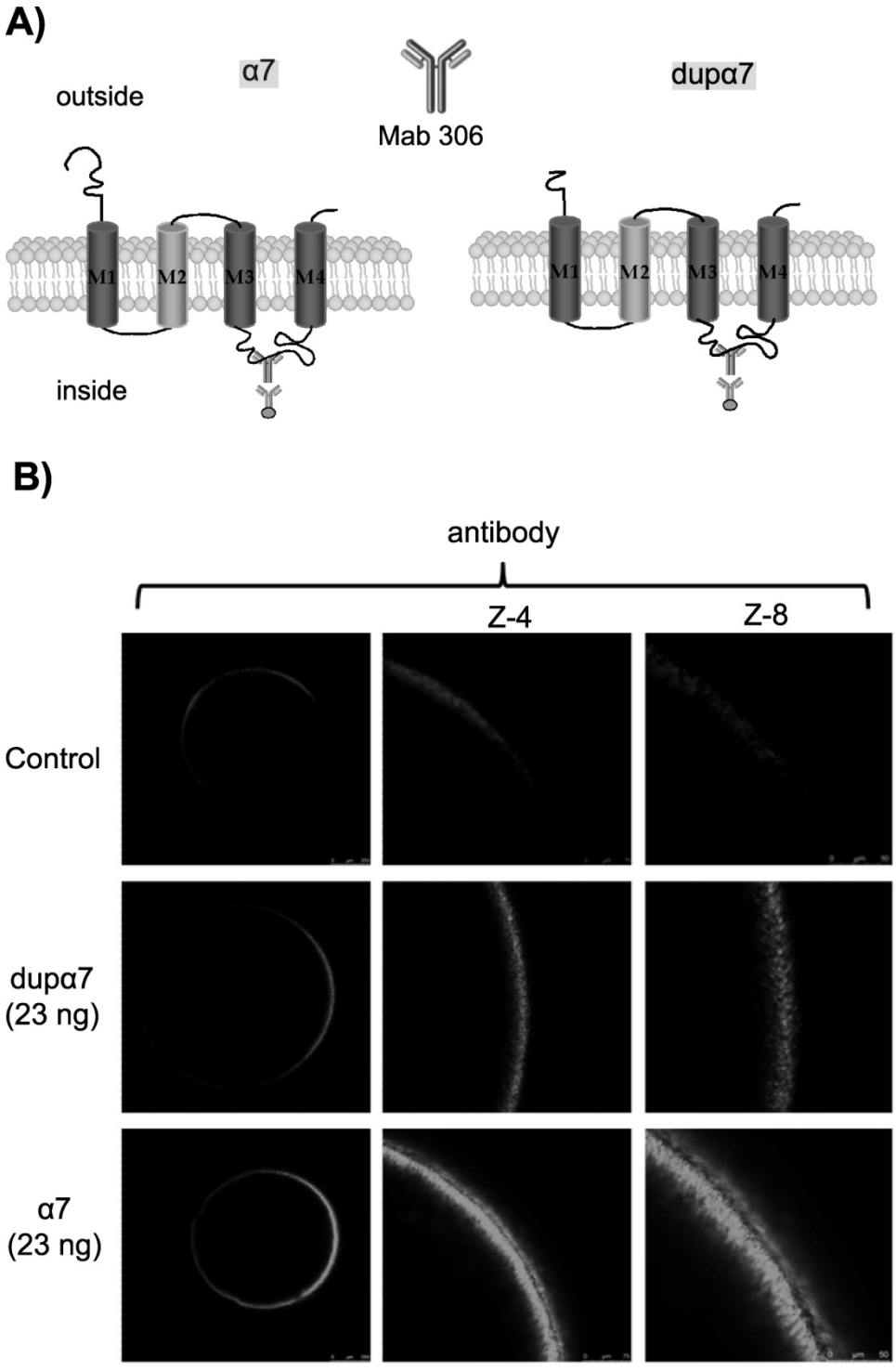
A)
α7
outside
Mab 306
dupα7
M1
M2
M3
M4
inside
B)
antibody
Z-4
Z-8
Control
dupα7
(23 ng)
α7
(23 ng)

Figure 2

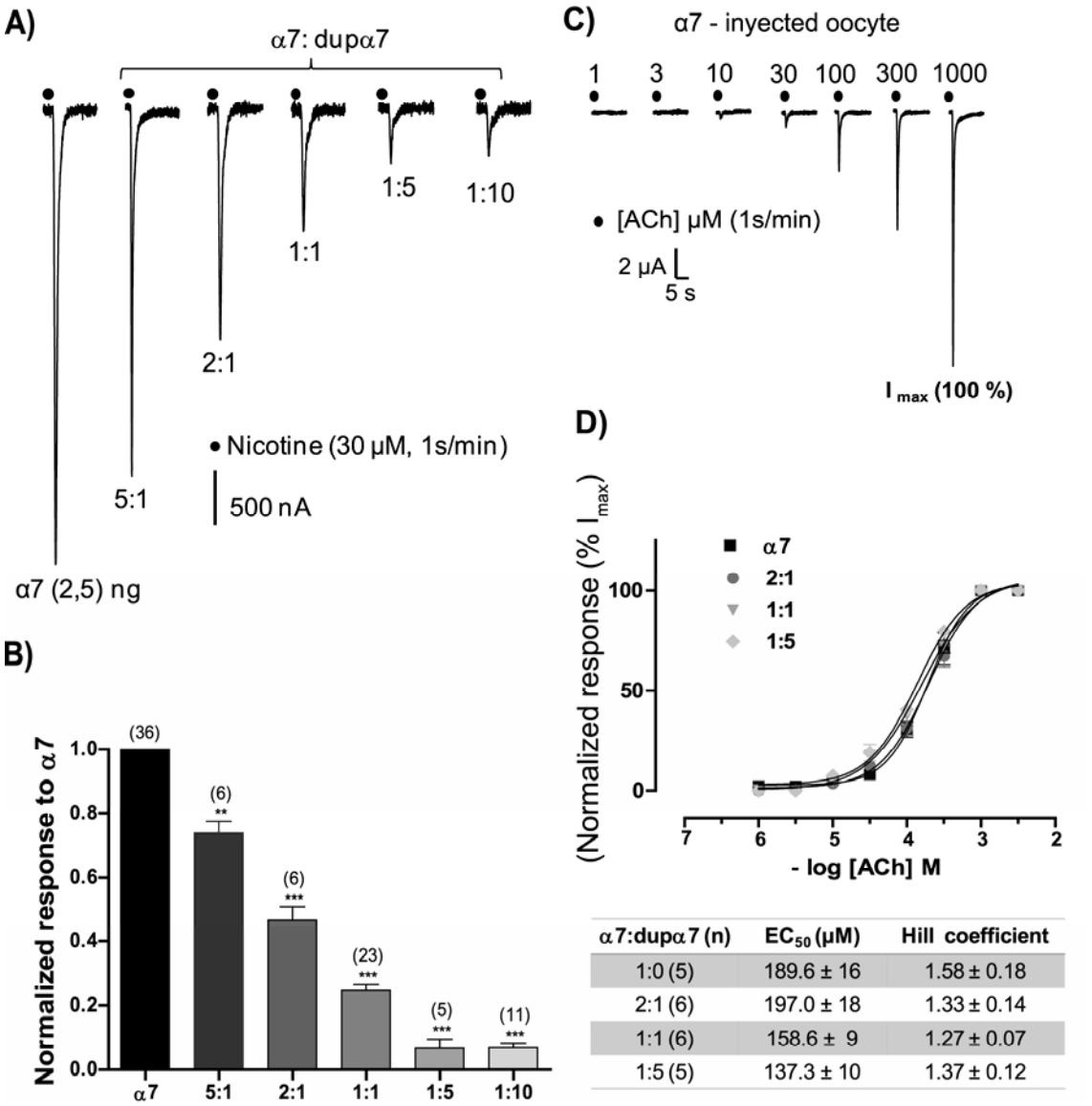

α7:dupα7 (n)	EC_{50} (µM)	Hill coefficient
1:0 (5)	189.6 ± 16	1.58 ± 0.18
2:1 (6)	197.0 ± 18	1.33 ± 0.14
1:1 (6)	158.6 ± 9	1.27 ± 0.07
1:5 (5)	137.3 ± 10	1.37 ± 0.12

Figure 3

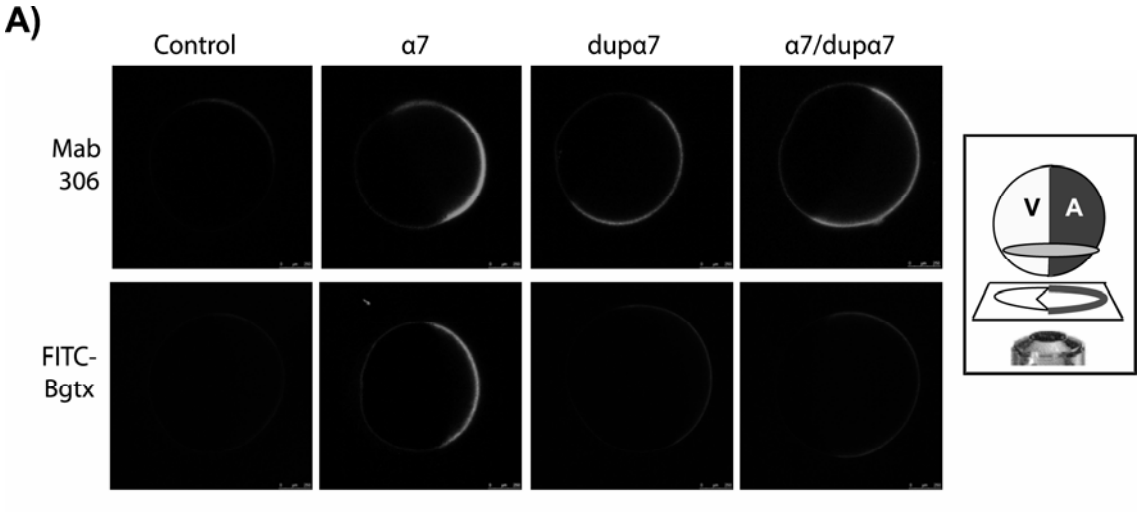

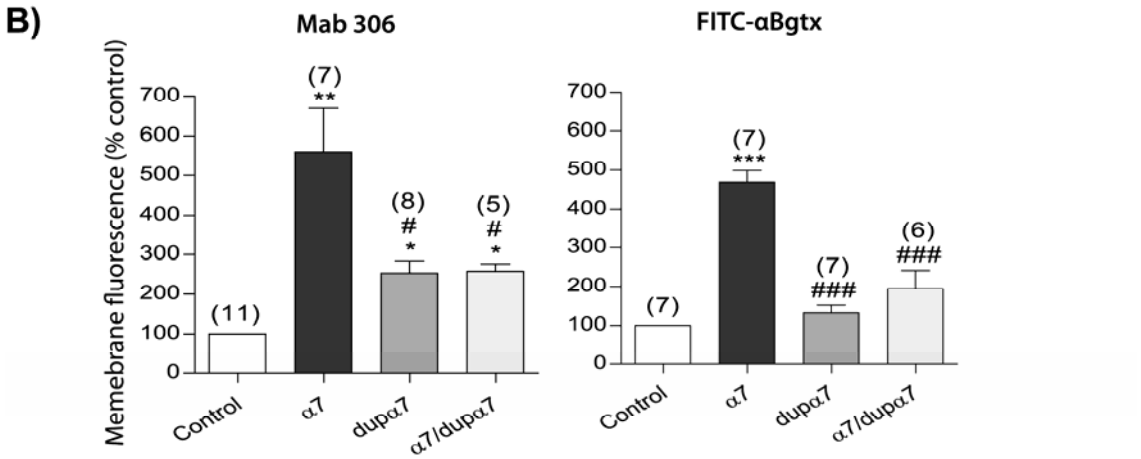

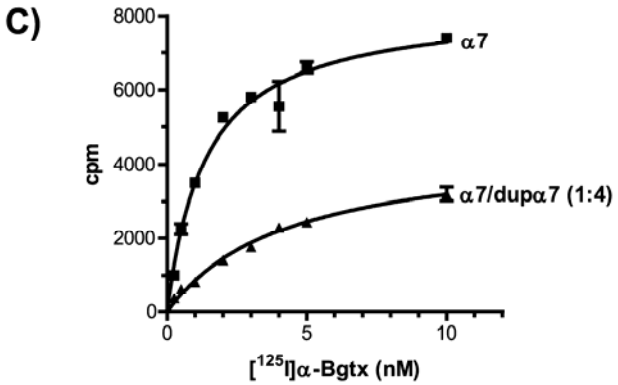

	α7	α7:dupα7 (1:4)
Kd (nM)	1.37 ± 0.17	4.28 ± 0.56 *
Bmax (cpm)	8277 ± 331	4552 ± 288 **

Figure 4

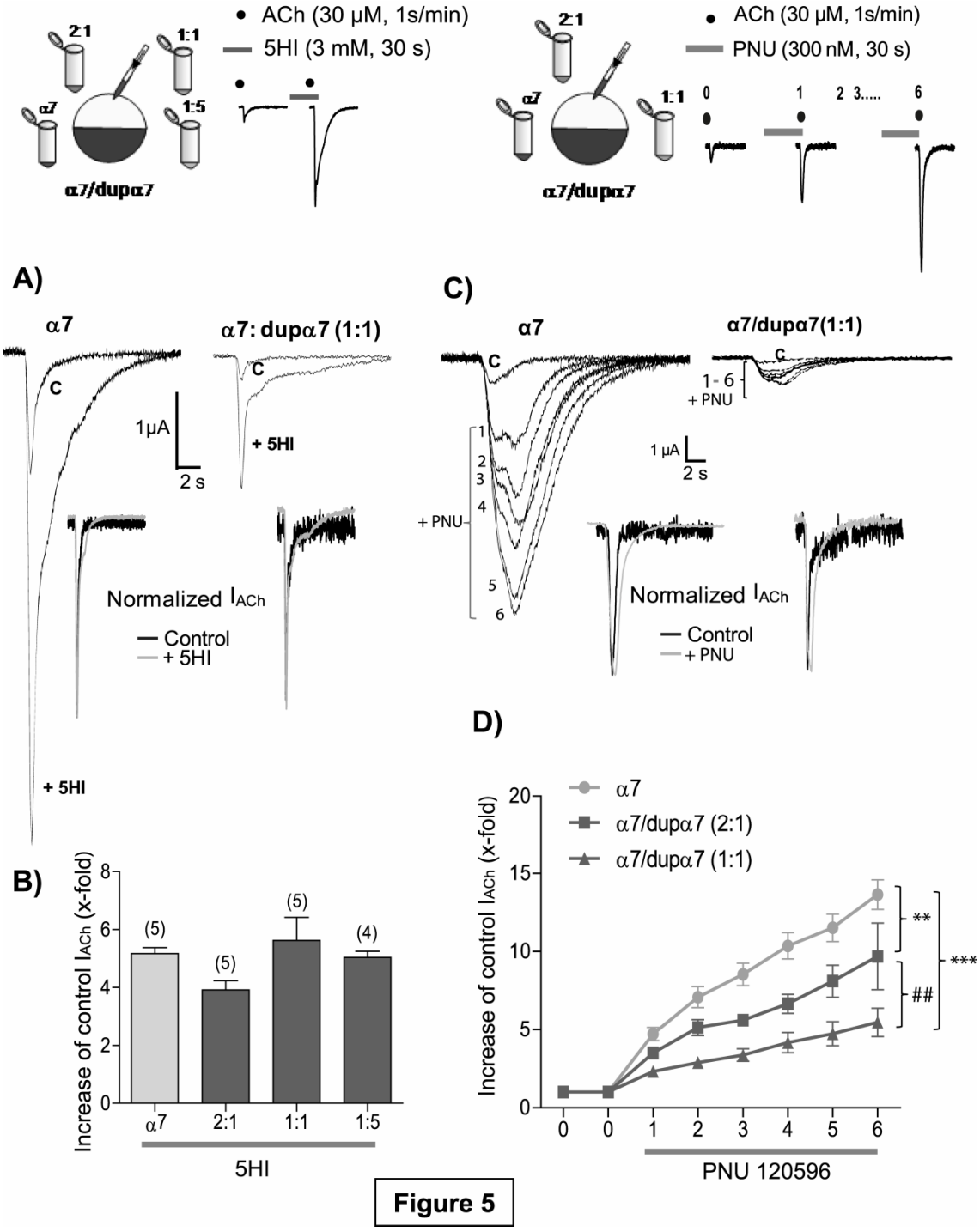
ACh (30 µM, 1s/min)
5HI (3 mM, 30 s)
2:1
1:1
1:5
α7
α7/dupα7
ACh (30 µM, 1s/min)
PNU (300 nM, 30 s)
0
1
2 3.....
6
A)
α7
α7: dupα7 (1:1)
C
1µA
2 s
+ 5HI
Normalized IACh
Control
+ 5HI
C)
α7
α7/dupα7(1:1)
1 - 6
+ PNU
1 µA
2 s
+ PNU
Normalized IACh
Control
+ PNU
B)
Increase of control IACh (x-fold)
(5)
(5)
(5)
(4)
α7
2:1
1:1
1:5
5HI
D)
α7
α7/dupα7 (2:1)
α7/dupα7 (1:1)
Increase of control IACh (x-fold)
**
##
***
PNU 120596

Figure 5

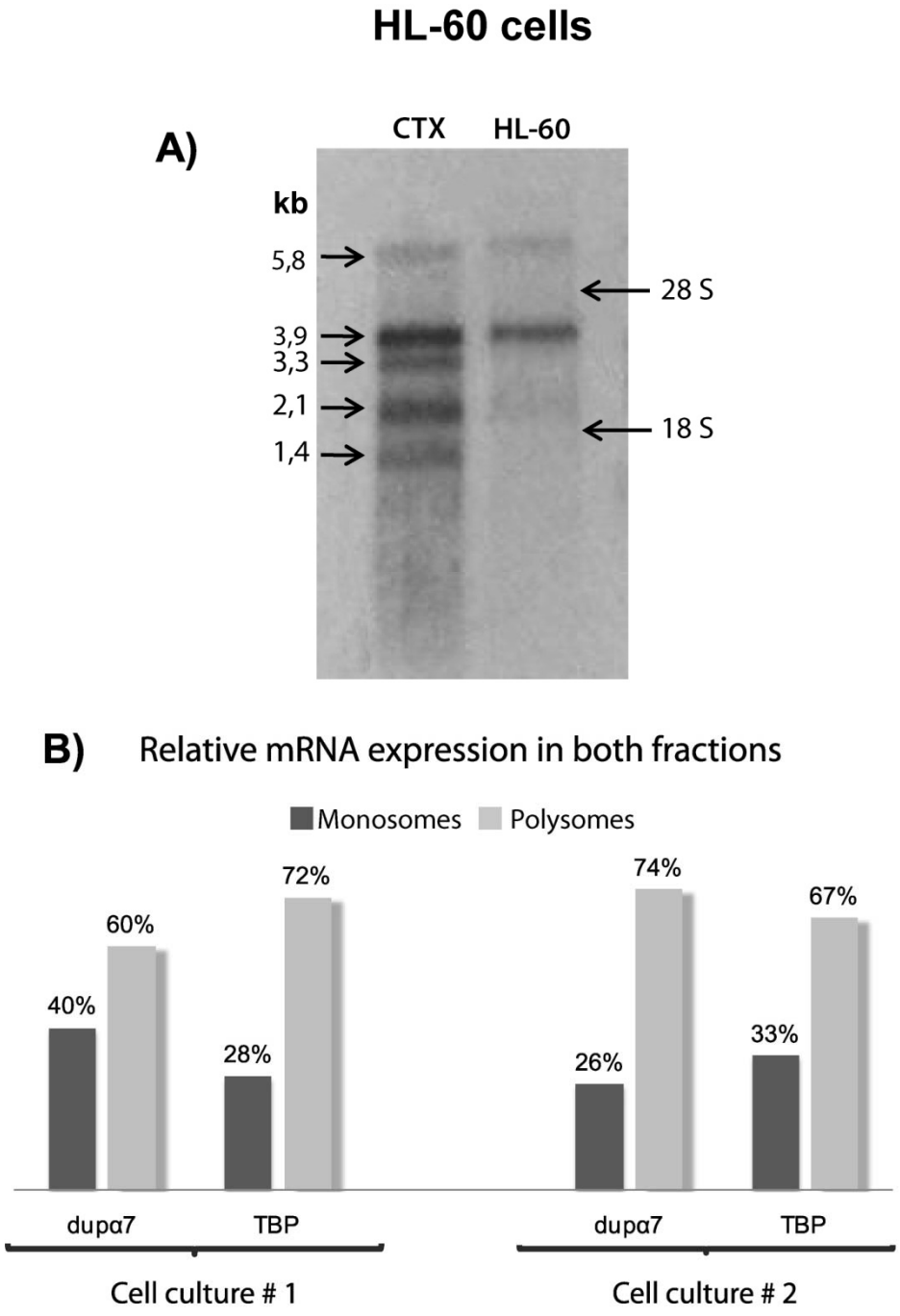
HL-60 cells
A)
CTX
HL-60
kb
5,8
3,9
3,3
2,1
1,4
28 S
18 S
B)
Relative mRNA expression in both fractions
Monosomes
Polysomes
40%
60%
28%
72%
26%
74%
33%
67%
dupα7
TBP
dupα7
TBP
Cell culture # 1
Cell culture # 2

Figure 6

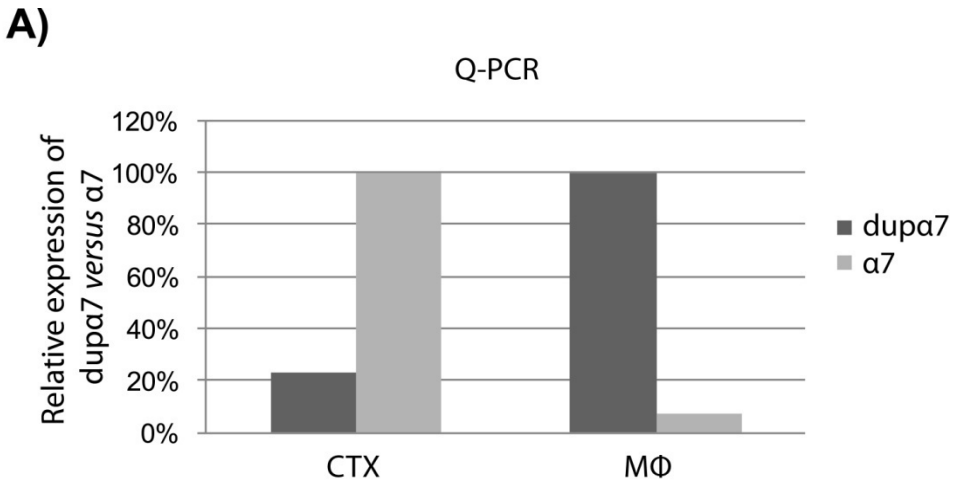
A)
Q-PCR
Relative expression of dupα7 versus α7
120%
100%
80%
60%
40%
20%
0%
CTX
MΦ
dupα7
α7

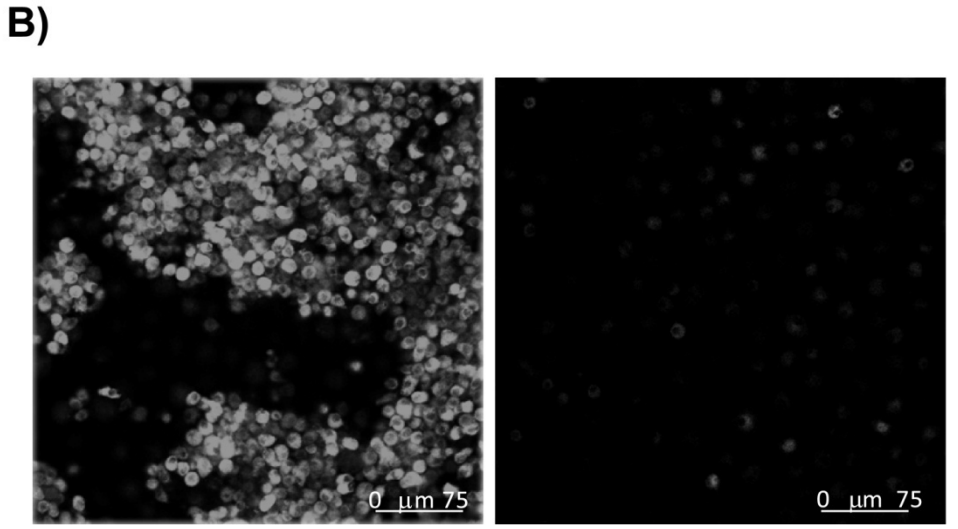
B)
0 µm 75
0 µm 75

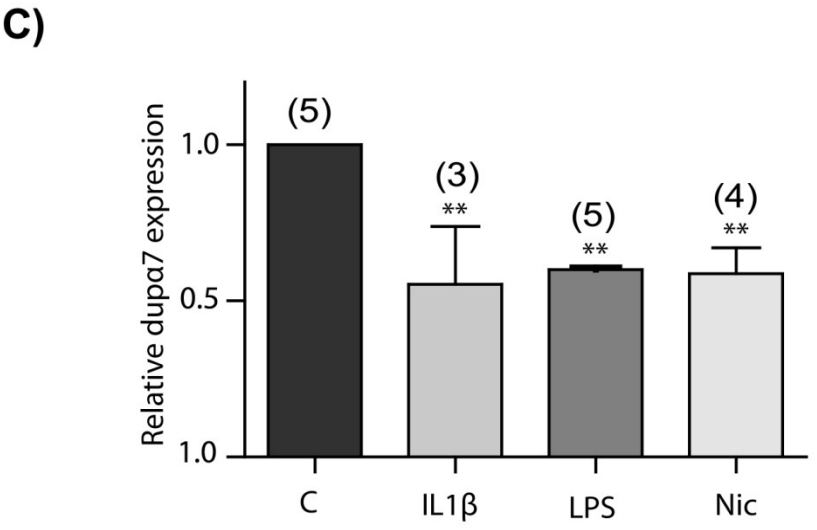
C)
Relative dupα7 expression
1.0
0.5
1.0
(5)
(3)
**
(5)
**
(4)
**
C
IL1β
LPS
Nic

Figure 7